DEPENDENCE OF THE DIFFRACTION ANGLES OF THE EDGE LIGHT BEAMS ON THE DISTANCE BETWEEN INITIAL THEIR TRAJECTORIES AND THE STRAIGHT EDGE OF A THIN SCREEN

Yu.I. Terent'ev

Institute of Atmospheric Optics,
Siberian Branch of the Russian Academy of Sciences, Tomsk
Received July 2, 1998

Deflection of light beams is studied in the deflection zones existing above a screen surface. The beam deflection angles are analyzed experimentally. The angles, by which edge beams deflect, are found depending on the distance between the layer in the deflection zone, where they deflect, and the straight edge of a thin screen.

Reference 1 presents the new experimental evidence of existence of the special zone above a body's surface, where light beams deflect in both directions from their initial trajectory. It is established that incident beams deflect by smaller angles as the layer in the deflection zone where they deflect moves farther apart from the screen. This deflection is shown to be the main cause for occurrence of the edge light (boundary wave). According to Ref. 2, the largest experimentally observed width of the deflection zone is about 70 μm.

This paper presents the results of research into the angles ε of light beam deflection in the deflection zone of a thin screen with a straight edge as functions of the distance h_z between the initial beam trajectories and the edge of the diffracting screen.

The experiment geometry is shown in the Fig. 1, where S is the 30-μm wide slit; S' is its image; *obj.* is the objective lens with the focal length of 50 mm; Scr_1 and Scr_2 are the thin screens (blades) with straight edges; W is the 20-mm wide window at PMT input; curve *1* characterizes rough distribution of light intensity over the width of S'; sl_0 is the 1.75-mm wide slit set in front of the objective lens.

The slit S is illuminated with the parallel beam of green light at $\lambda = 0.53$ μm. This light beam is separated out from radiation of the filament lamp with the interference filter. The screen Scr_1 is set in the plane of S'. To obtain the maximal light flux Φ_2 of the edge light behind the screen Scr_1, its edge is set in the center of S' based on attenuation of the light flux of beams forming S' to 0.5 of the total light flux Φ_{inc}.

The right screen of sl_0 limits the light flux at the level $\min_1$ of the diffraction pattern of S in the front focal plane of the objective lens. The left screen of sl_0 cuts off rays of the left half of the beam in order to prevent illumination of the area behind Scr_1 without light deflection in the Scr_1 deflection zone. When the left part of the beam is cut off by the left screen of sl_0, most intense rays of the beam, which are parallel to its axis, find themselves at the edge of the beam. As a result, the edge beam formed by them in the area shadowed by the screen Scr_1 becomes detectable at small diffraction angles. Consequently, it becomes possible to study the edge light in the wider range of deflection angles than in Ref. 1. Besides, larger widths of the deflection zone can be found. The width of S' equals 70 μm, when the light flux passing through it is 0.92 of the total incident beam flux. The input window W is set at the distance $L = 100.6$ mm from the plane of Scr_1.

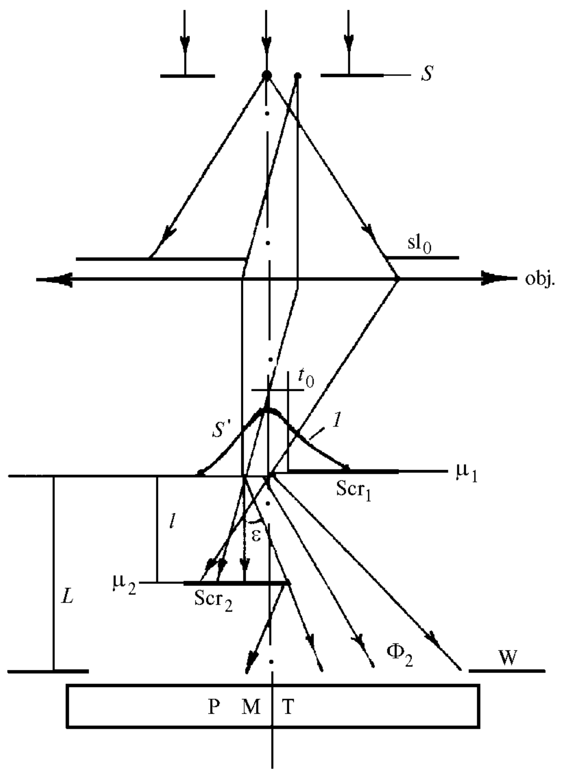

FIG. 1. Geometry of the experiment on research into the edge light propagating in the shadow area of the screen Scr_1.

0235-6880/98/12 1088-05 $02.00

In the experiments, the edge light resulting from deflection of the incident beam in the Scr_1 deflection zone in the direction to Scr_1 was attenuated with the screen Scr_2 as the latter moves in the direction of the Scr_1 shadow. The value of Φ_2 expressed in percent of Φ_{inc} was kept constant in the experiment. Under these conditions the gap t between the projections of Scr_1 and Scr_2 upon the plane normal to the beam axis (or the distance r, by which the screen Scr_1 goes beyond the screen Scr_2) was measured at different distances l between the screens (Fig. 2).

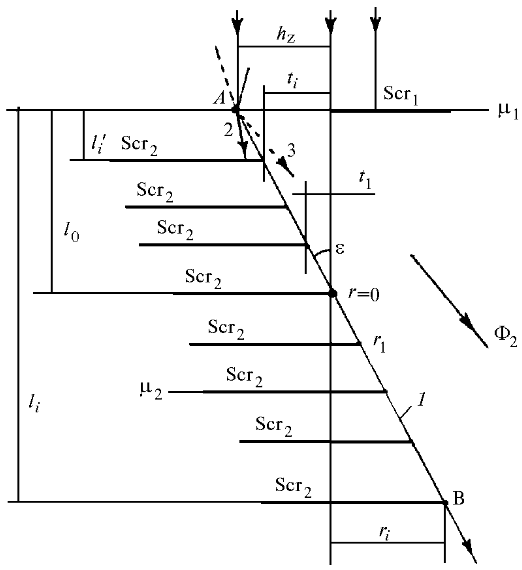

FIG. 2. Geometry of the experiment for determination of the deflection angles of the light beams deflected in the Scr_1 zone at different distances h_z measured from Scr_1.

Prior to the experiment, we have found the position of the S' axis by the maximum value of the light flux having passed through the slit. The micron-wide slit was formed by the screen Scr_1 and the auxiliary screen put to its left. As a result, we has found that while the flux in the plane of S' falls down to 0.5 Φ_{inc}, the edge of Scr_1 does not approach the axis of S' by t_0 = 3.5 μm (see Fig. 1). The cause for this is likely the following. The total light flux of the incident beam before its splitting into edge light beams deflected in both directions exceeds the combined flux after beam splitting due to a phase shift between parts of the beam. Consequently, the light flux from the open half of S' turns out to be less than 0.5 Φ_{inc}.

According to the above-said, if Scr_1 and Scr_2 are set at such positions that each of them separately attenuates the light flux to 0.5 Φ_{inc}, then the gap between them is $2t_0$ = 7 μm.

Table I presents the values of t and r versus l for the case when the light flux Φ_2 of the edge light is attenuated by the screen Scr_2 down to 8.5% of Φ_{inc}.

TABLE I.

l, mm	t, μm	r, μm
0.3	8.5	–
0.6	7.6	–
1.01	6.1	–
1.55	2.9	–
2.04	0	0
2.05	–	0.07
2.45	–	2.42
3	–	5.7
3.45	–	8.3
3.95	–	11.25
4.45	–	14.1

These values were obtained in the following way:

1. Reading $l_{2.0}$ of the micrometer μ_2 was taken for the case, when the light flux was screened with the screen Scr_2 so that its value fell to 0.5 Φ_{inc}.

2. The light flux attenuated by the screen Scr_1 down to 0.5 Φ_{inc} (the maximum value of Φ_2) was then attenuated by the screen Scr_2 to the value Φ_2 = 8.5% of Φ_{inc}. Reading $l_{2.1}$ corresponded to this position of the screen Scr_2.

The readings $l_{2.0}$ and $l_{2.1}$ were then used to determine

$$t, r = [(M_{2.1} - M_{2.0}) - 2\,t_0].$$

The plot of the function $t, r = f(l)$ drawn based on the data from Table I is the straight line at $l \geq 1$ mm (Fig. 3).

Consequently, for the case $l \geq 1$ mm the edge of the screen Scr_2 at different l and the same attenuation of Φ_2 lies at the straight line AB (see Fig. 2). This line is just the propagation path of the edge beam *1*, which is least deflected in the deflection zone of the screen Scr_1 in the direction to it. This edge of the screen Scr_2 limits the edge light flux Φ_2 from small deflection angles of edge beams.

The efficiency of light deflection in the deflection zone drops in the direction from the screen to the outer boundary of the zone. So, evidently, the least deflected rays passing near the Scr_2 edge were deflected in the Scr_1 deflection zone at some point at a distance h_z from the Scr_1 edge, rather than at the edge itself. These rays come from the level corresponding to the point A situated at the intersection of the boundary ray with the extension of the plane of Scr_1.

The boundary ray *1* coming from the largest h_z at a given attenuation of Φ_2 is the extension of the ray parallel to the beam axis, because the slant rays *2* deflected at the level A by the same angle are cut off by the screen Scr_2, and the rays *3* are screened by the left screen of the slit sl_0.

This circumstance allows us to determine the deflection angles ε of the boundary edge rays by measuring them from the line parallel to the incident beam axis.

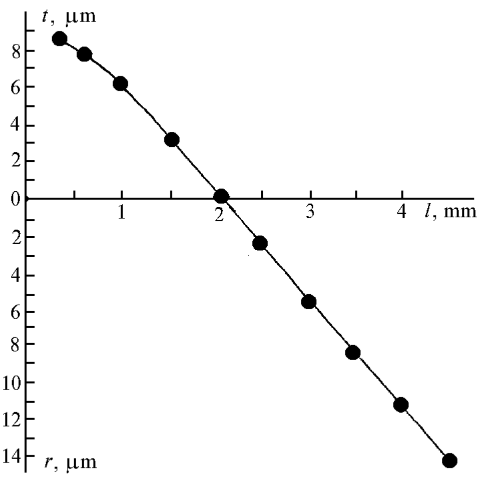

FIG. 3. The gap t between the two screens Scr_1 and Scr_2 set in series or the distance r, by which one screen goes beyond the another, as a function of the distance between the screens, while the second screen attenuates the edge light flux coming from the first screen down to 8.5% of the incident light flux.

Since the left screen of the slit sl_0 cuts off the slant rays *3*, the total light flux passing between the screens Scr_1 and Scr_2 originates from the layer with the width h_z of the Scr_1 deflection zone.

Because the line *AB* is straight, h_z and ε can be found from the following expressions:

$$h_z = r_i \, l_0/(l_i - l_0), \tag{1}$$

$$h_z = \{[(r_i - r_{i-m}) \, l_{i-m}/(l_i - l_{i-m})] - r_{i-m}\}, \tag{2}$$

$$h_z = \{[(t_i + r_i) \, l'_i/(l_i - l'_i)] + t_i\}; \tag{3}$$

$$\varepsilon = \frac{h_z}{l_0} = \frac{r_i - r_{i-m}}{l_i - l_{i-m}} = \frac{h_z - t_i}{l'_i} \,. \tag{4}$$

It is easy to understand that the less attenuated is the edge light flux Φ_2 by the screen Scr_2, the wider is the layer h_z of the Scr_1 deflection zone, from which this light flux originates and the smaller are deflection angles of the boundary rays, and vice versa.

TABLE II.

Φ_2*, %	l'^{**}_i, mm	l^{**}_{i-m}, mm	l^{**}_i, mm	t^{***}_i, µm	r^{***}_{i-m}, µm	r^{***}_i, µm	h_z, µm	ε, min. of arc	ε_{calc}, min. of arc	Φ_2, rel. units
12.93	–	3.45	4.45	–	0	4.57	15.75	15.7	15.7	109.4
8.53	–	2.05	3.95	–	0.066	11.25	12	20.24	20.2	72.2
6	1.01	–	3.95	1.987	–	20.125	9.583	25.9	25.03	50.76
4	–	1.01	3.95	–	2.07	29.93	7.5	32.6	31.3	33.84
2	–	1.01	3.95	–	10.145	52.63	4.45	49.68	49.56	16.92
1	–	1.01	3.95	–	20.145	86.23	2.56	77.27	77.55	8.46
0.5	–	1.01	3.95	–	33.47	135	1.407	118,73	118,32	4,23
0.296	–	1.01	3.95	–	44.33	176	0.9	153.9	154	2.5

* The values of Φ_2 are given in percent of Φ_{inc}.
** The values of l used to determine h_z and ε at a given attenuation of Φ_2.
*** t_i, r_i, r_{i-m} are the values of t and r at the corresponding l' and l.

Table II presents the values of h_z and ε determined by Eqs. (1)–(4) with different attenuation of the flux Φ_2 by the screen Scr_2.

The h_z dependence of ε is shown in Fig. 4. The analysis of this dependence has revealed that as h_z varies from 0.9 to 16 µm

$$\varepsilon = 259.5/(h_z + 0.786), \tag{5}$$

$$h_z = (259.5 - 0.786 \, \varepsilon)/\varepsilon, \tag{6}$$

where ε is expressed in minutes of arc and h_z is expressed in micrometers.

The validity of these equations can be easily checked by comparing the diffraction angles ε calculated by Eq. (4) and presented in Table II with values of the diffraction angles ε_{calc} calculated by Eq. (5).

If the expression (5) is assumed also true at $h_z > 16$ µm, then the rays coming from the distance of 70 µm from the screen[2] are deflected by ε = 3.7′; the rays coming from $h_z = 60$ µm are deflected by 4.3′, i.e. by the critical angle[3]; and the rays coming from $h_z = 259$ µm are deflected by 1′. For the case of $h_z = 0$, ε = 5.5°. In actual practice, weak edge light is observed even at ε > 21°. Its existence can be explained by scattering of the incident light at a curvature of the screen (blade) edge and possible violation of the validity of Eq. (5) for $h_z < 0.9$ µm.

At $h_z \gg 0.786$, the almost inversely proportional dependence establishes between ε and h_z.

In the experiments aimed to prove the existence of the deflection zone[1] with $h_z = 4.7$ µm, the edge rays deflected by 49′. According to Eq. (5), $h_z = 4.7$ µm corresponds to $\varepsilon = 47.3'$. As seen, the earlier obtained results agree well with Eq. (5).

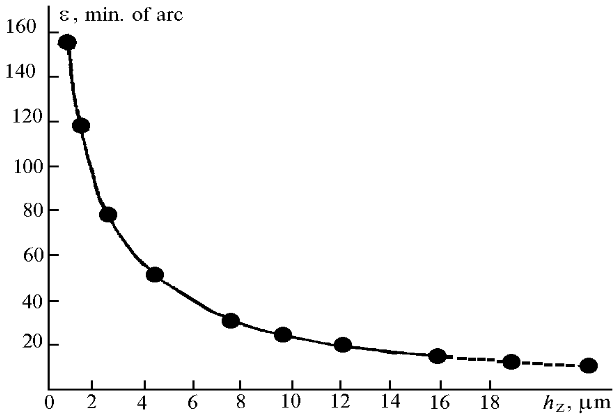

FIG. 4. Deflection angles ε of the edge rays vs. the distance h_z between their initial trajectories and the diffracting screen.

The authenticity of the tabulated values of h_z is confirmed by the smooth run of the plotted dependence $\Phi_2 = f(h_z)$ to the origin of coordinates in Fig. 5.

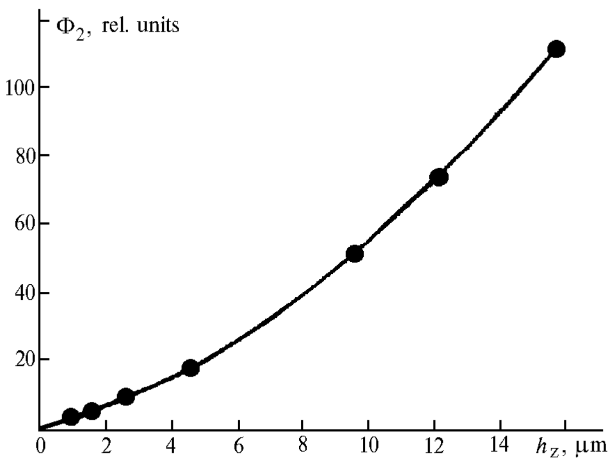

FIG. 5. The edge light flux Φ_2 coming from the layer h_z of the Scr_1 deflection zone into the shadow area of Scr_1 and Scr_2 vs. the layer width.

The curvature of the plot can be explained as follows. While r decreases by Δr, Φ_2 grows not only due to expansion of the section of the deflection zone, light from which comes through Scr_1 and Scr_2 to Δh_z, but also because the screen Scr_2 goes away from the path of the slant rays *2* deflected at the previous section of the deflection zone.

References 3–5 experimentally prove the formation of diffraction pattern from a screen due interference of the edge light with the directly passing light. This allows us to determine h_z as a function of ε using the experiments with the geometry shown in Fig. 6.

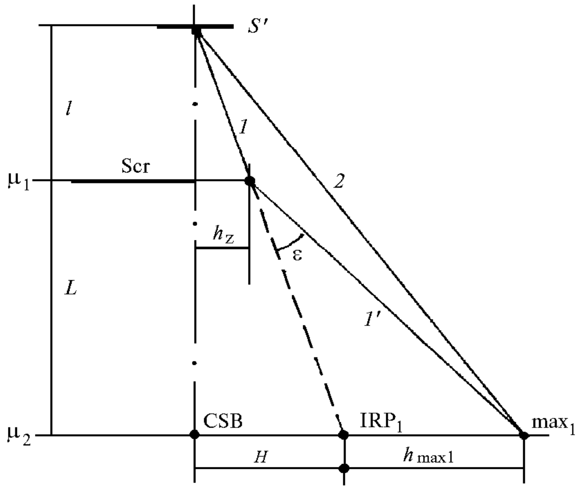

FIG. 6. Geometry of light diffraction on the screen. CSB is the classical shadow boundary[4]; IRP_1 is the projection of the incident ray 1, which turns into the ray 1' after deflection in the deflection zone of the screen Scr at a distance h_z from Scr (this ray comes to the point $\max_1$*); the ray 2 is the straight ray interfering with the ray 1' without propagation difference; μ_2 is the micrometer screw moving the scanning slit; h_{max1} is the distance from* $\max_1$ *to IRP_1; m is the distance between IRP_1 and CSB.*

According to Eq. (1) (Ref. 4)

$$h_{max1} = [2\lambda\, L\, (L + l)/l - h_{21}^2]/2\, h_{21},$$

where h_{21} is the distance between the first maximum and the second one. As follows from the geometry,

$$\varepsilon = h_{max1}/L;\ h_z = Hl/(L + l).$$

In the experiments the edge of the screen *Scr* was set on the axis of the cylindrical beam by halving of the beam light flux. The point halfway between the points with equal light intensity in the left and right parts of the beam with the screen removed was taken as a projection of the axis upon the scanning plane of the diffraction pattern, just which is CSB. The position of IRP_1 was determined by h_{max1}.

Table III compares the values of h_z for the same ε calculated by Eq. (6) (h_{z1}) and those found from experiments on light diffraction on a screen (h_{z2}). The close values of h_z for both cases are the additional confirmation for the validity of Eq. (5).

Let us express h_z in millimeters and ε in radians in Eq. (6). Then

$$h_z = (0.0755 - 0.786\, \varepsilon)/1000\, \varepsilon.$$

Let us replace ε with Δε and find the corresponding Δh_z: $\Delta h_z \approx 0.0755\Delta\varepsilon/1000\, \varepsilon^2$. In this case $\Delta h_z/\Delta\varepsilon = 7.55 \cdot 10^{-5}/\varepsilon^2$. At constant intensity of the incident light throughout the width of the deflection zone, the intensity J of the edge light coming from Δh_z is inversely proportional to $\Delta\varepsilon$ at the point of observation. Consequently, it is inversely proportional to ε^2 as well. The same dependence between J and ε follows from Eq. (10) of Ref. 3, which relates the intensity of the edge light to that of the incident light J_c:

$$J_b = 0.0205\ \lambda\ L\ J_c/h^2.$$

TABLE III.

Screen	λ, μm	l, mm	L, mm	h_{max1}, mm	H, μm	ε, min of arc	h_{z1}, μm	h_{z2}, μm
Blade	0.53	6	99.5	0.715	140	24.7	9.8	8
“	“	“	“	0.71	138	24.5	9.9	7.9
“	“	12	“	0.571	85	19.7	12.7	9.2
“	“	≪	“	0.583	131	20.14	12	14.1
“	“	≪	“	0.536	118	18.5	13.4	12.7
“	0.6328	11,4	“	0.688	112	23.8	10.3	11.5
“	0.53	12	“	0.555	117	19.2	12.8	12.6
“		“	“	0.565	110	19.5	12.7	11.9
“		22	“	0.438	88	15.1	16	15.9
“		24	“	0.412	85	14.6	16.7	16.5
“		22	“	0.442	101	15.3	15.9	15.6
“		35.5	“	0.372	89	12.9	20	21.4
Aluminum bar ∅5.8 mm	“	38.4	96.6	0.345	74	12.3	20.3	21
Steel cylinder ∅30 mm	“	35.5	98.5	0.363	70	12.7	19.7	18.5
Blade	“	52.5	99.5	0.327	66	11.3	22.2	22.8
“	“	“	“	0.321	53.5	11.1	22.6	18.5
“	“	90	“	0.260	68.5	9	28	32.5

To be certain, let us transform it by multiplying and dividing h^2 by L^2 to the form

$$J_b = 0.0205\ \lambda\ J_c/L\ \tan^2\varepsilon \approx 0.0205\ \lambda\ J_c/L\ \varepsilon^2.$$

The same dependence of J_b on ε in both equations is one more evidence of validity of Eq. (6).

In conclusion, we note that the established regularities are the new confirmation of real existence of deflection zones above surfaces of bodies (screens) and the validity of the Young concepts about the cause for formation of light diffraction patterns.

REFERENCES

1. Yu.I. Terent'ev, Atmos. Oceanic Opt. **8**, No. 4, 262–268 (1995).
2. Yu.I. Terent'ev, Atmos. Oceanic Opt. **6**, No. 4, 214–216 (1993).
3. Yu.I. Terent'ev, Atm. Opt. **2**, No. 11, 975–981 (1989).
4. Yu.I. Terent'ev, Atmos. Oceanic Opt. **9**, No. 3, 202–208 (1996).
5. Yu.I. Terent'ev, Atm. Opt. **2**, No. 11, 970–974 (1989).